



# Population synthesis for the spectra of blue compact dwarf galaxies<sup>†</sup> \*

KONG Xu<sup>1,2,3</sup> CHENG Fu-zhen<sup>1,2</sup> ZHOU Xu<sup>2,3</sup> CHEN Jian-sheng<sup>2,3</sup>

<sup>1</sup>Centre for Astrophysics, University of Sciences & Technology of China, Hefei 230026

<sup>2</sup>National Astronomical Observatories, Chinese Academy of Sciences, Beijing 100012

<sup>3</sup>CAS-Peking University Joint Beijing Astrophysical Center, Beijing 100871

**Abstract** In order to study the history of star formation, energy source and internal dust distribution in blue compact dwarf galaxies (BCDGs), we have compared the observed spectra of the nuclei of 7 BCDGs with the predictions of stellar population synthesis model. The results suggest that BCDGs are old galaxies, in which star formation occur in short intense bursts separated by long quiescent phases. The star formation rate was very high during  $5 \times 10^7 \sim 10^9$  yr, but has now decreased. We find that the main energy source of BCDGs comes from young, massive stars. We have derived the internal reddening that affects the nuclear stellar population by the population synthesis method and the internal reddening of the emitting gas clouds from the Balmer line ratio and found the former to be consistently and significantly smaller than the latter. This feature can be explained by a model of foreground dust clumps with different covering factors for the gas and stars. Finally, based on the stellar population of BCGs (blue compact galaxies) and BCDGs, we suggest a detailed evolutionary link among different dwarf galaxies.

**Key words:** blue compact dwarf galaxies—population synthesis—internal reddening—star formation

## 1. INTRODUCTION

Blue compact dwarf galaxies (BCDGs) are tiny objects that are dominated by intense star formation. The star formation process and surrounding conditions are different from our

<sup>†</sup> Supported by National Natural Science Foundation (No. 19473010), the National Pandem Project and the Very Important Project of CAS (KJ951-A1-302)

Received 1999-02-01; revised version 1999-04-23

\* A translation of *Acta Astrophys. Sin.* Vol. 19, No. 4, pp. 380–392, 1999

Galaxy and other nearby galaxies<sup>[1]</sup>. They were first observed and studied by Zwicky et al.<sup>[2-4]</sup>. Photometric observations of these galaxies are characterized by small physical sizes (1-3 kpc), very low luminosity ( $-14 \geq M_B \geq -20$  mag), and disorderly distributions of HII regions from photoionization by massive stars<sup>[5-7]</sup>. As their name suggests, BCDGs have very blue UBV colors ( $(B - V) \sim 0.22, (U - B) \sim -0.6$ )<sup>[6]</sup>. Most of them have no companion galaxies. Radio observations at 21 cm have revealed the presence of large quantities of neutral hydrogen in BCDGs<sup>[8]</sup>. Their optical spectra show strong narrow emission lines superposed on a nearly featureless continuum, similar to the spectrum of HII region<sup>[9]</sup>. In  $\sim 10\%$  of BCDG spectra, there exists the HeII $\lambda$ 468.6 nm line at the blue end, implying the presence of many massive, ionizing WR stars. Their near infrared spectra indicate the existence of some red-giant stars<sup>[5]</sup>. The blue colors and strong emission lines indicate that violent bursts of star formation are taking place inside these galaxies, and lots of massive, hot stars are formed. These hot stars ionize the interstellar material and form the high ionization HII regions that produce the strong narrow emission lines. Their ultraviolet spectra are characterized by a stellar continuum from early-type O, B stars that rapidly rises blueward and shows a distinct UV excess<sup>[4]</sup>. Systematic spectroscopic studies of BCDGs have shown that their metallicity is low, less than or equal to the metallicity of the sun<sup>[10]</sup>.

Intense bursts of star formation give birth to a large number of massive stars in compact regions, which ionize the interstellar medium, enrich it with heavy elements, and cause rapid changes in the elemental abundances. Moreover, these intense bursts of star formation make the star forming regions radiate strongly over much of the electromagnetic spectrum, and allow an accurate determination of the elemental abundance in the ionized gas. These properties make BCDGs most suitable for studying the relative variations of the chemical elements and the chemical evolution of the galaxies, and for constraining the stellar nuclear synthesis model and determining the initial mass function of stars<sup>[11]</sup>. Moreover, BCDGs are the least chemically evolved galaxies known, containing very little heavy elements manufactured by stars after the big bang, so can be used for a determination of the primordial helium abundance  $Y_p$  and verification of the theory of cosmic origin<sup>[12]</sup>. Free of spiral density waves, the BCDGs are fit for studying the formation mechanism of star in galaxy<sup>[6]</sup>. Now, following the development of observing techniques, more and more astronomers are beginning to study the properties of these objects. Because the star formation is extremely violent, the rate of star formation is high, so the neutral hydrogen in the interior will have been burnt within a short timescale. Hence, the most common interpretation for the low metallicity and high star formation rate is that BCDGs are young objects, and that they are being seen at the phase of the formation of the first generation stars. However, some recent observations find that there exist some old stellar populations in them; thus, their age is still an open question<sup>[13]</sup>.

In addition, we have little knowledge about the effect of internal reddening in BCDGs, and a unified extinction law is yet to be found. The difficulty is that we are not clear about the physics, chemistry and geometrical distribution of the interstellar matter inside these galaxies. Moreover, we do not know how sensitive these external galaxies are to their internal dust distribution. Also, we must think about the re-emission from dust absorption<sup>[14]</sup>.

The main observational characters of BCDGs are determined by the character and evolution of the stars in their interior. When we study the energy source, spectral energy

distribution, physical condition and chemical evolution of BCDGs, the first and most critical step is an investigation of the internal dust distribution and the stellar population. Once we resolve the stellar population, we will know their main characters. Because of observational limitations, we can not resolve individual stars in the compact regions of BCDGs. In order to determine the properties of BCDGs, we applied the population synthesis method based on star cluster integrated spectra (developed by Bica et al.) to 7 BCDG optical spectra in this paper. This is capable of yielding the various stellar components, the internal reddening and the history of the star formation. And finally we can get the true spectrum of the emission line region after subtracting the model stellar population spectrum from the observed spectrum.

## 2. OBSERVATIONS AND DATA REDUCTION

Our sample of 7 blue compact dwarf galaxies was selected from the emission line galaxy catalog of Kinney et al.<sup>[7]</sup>. Long-slit, high S/N spectroscopic observations were carried out in 1997 March 18–20. All the observations were made with the 2.16-m telescope at the Xinglong Station of Beijing Astronomical Observatory, using a Zeiss universal spectrograph with a grating of 300 grooves/mm dispersion. A Tek 1024×1024 CCD was used, covering a spectral range from 350.0 to 750.0 nm with a resolution of 1.0 nm. The slit aperture was fixed at 240  $\mu\text{m}$ , corresponding to 2.5'' on the sky (typical seeing at Xinglong Station is 2''). The basic parameters are listed in Table 1, where the successive columns give the name of the galaxy, its coordinates, morphological type, radial velocity relative to the Local Group, photographic magnitude, absolute magnitude, and the observation date and exposure time.

**Table 1** Parameters of the Blue Compact Dwarf Galaxies

Galaxy Name	$\alpha(1950)$ (h-m-s)	$\delta(1950)$ (d-m-s)	Morph. Type	$V_H$ (km/s)	$B_T$	$M_B$ $H_0 = 50$	Date-Obs. (dd/mm/yr)	Exp. (s)
NGC 2537	08:09:42.5	46:08:32	Sc	441	12.4	-18.13	18/03/1997	1200
Mrk 19	09:12:53.5	59:58:53		4230	15.6	-19.07	18/03/1997	1800
Mrk 108	09:17:26.1	64:26:57	IO	1534	15.4	-17.57	18/03/1997	2000
Mrk 25	10:00:22.0	59:40:50		2602	14.8	-18.96	19/03/1997	1500
Mrk 35	10:42:16.5	56:13:23	Im	995	13.2	-18.50	18/03/1997	1200
UGC 9560	14:48:55.1	35:46:36	Ir	1213	14.8	-17.95	18/03/1997	1500
UGCA 410	15:35:48.4	55:25:34	dE	665	15.4	-16.63	20/03/1997	2820

The standard reduction is made using the IRAF packages. We followed standard procedure in the data reduction: bias subtraction, flat fielding, sky subtraction, cosmic ray extinction, CCD response curve calibration, then we extracted the one dimensional spectrum for each BCDG. For each extracted spectrum, we calibrated its wavelength and flux first, and then corrected for the foreground reddening and redshift. The spectra were wavelength calibrated using a He/Ar comparison lamp, more than 20 lines were used to establish the wavelength scale. On most nights, two KPNO standard stars (from among sa29130, feige 34 and feige 98) were used to perform the relative flux calibration. The final extracted spectra of the BCDGs (labeled OBS) are displayed in Figure 1.

For the purpose of accurate measurement of the equivalent width of absorption lines and the internal reddening in continuum regions, we measured the fluxes in 5 continuum intervals (width 2.0 nm) that are far from strong emission and absorption lines, centered on the following wavelengths: 360.0, 402.0, 457.0, 587.0, 663.0 nm. Also, since the BCDGs show a clear Balmer discontinuity in the near ultraviolet, we also measured the fluxes (point values) at 378.4, 381.4, 386.6 and 391.8 nm. The measured fluxes are given in Table 2.

**Table 2** Average Fluxes at Selected Continuum Wavelengths

Name	366.0	378.4	381.4	386.6	391.8	402.0	457.0	587.0	663.0
NGC 2537	7.656	6.919	9.094	8.437	11.50	10.96	12.11	12.30	9.796
Mrk 19	4.501	4.262	6.930	9.890	7.892	6.419	5.059	3.586	3.107
Mrk 108	4.251	3.332	8.533	8.476	7.062	7.274	4.626	4.185	3.724
Mrk 25	27.24	27.56	30.09	34.52	34.11	33.14	29.87	24.76	21.54
Mrk 35	32.33	25.54	29.47	34.23	36.93	42.08	31.89	23.69	20.50
UGC 9560	32.92	39.65	42.89	49.00	47.51	41.58	36.54	25.78	21.37
UGCA 410	12.03	20.69	23.10	26.16	22.41	18.47	16.78	14.55	14.06

After fitting the 9 continuum points to a continuum spectrum, we measured the equivalent widths of seven characteristic absorption lines. Because these were to be used as criteria for population synthesis, their selection and wavelength ranges were chosen to be the same as in Ref. [15]. The results are given in Table 3, the unit is nm, and negative sign denotes emission lines. The name of the line and the corresponding wavelength range are given in the first two columns, the equivalent widths are given in the successive columns.

**Table 3** Equivalent Widths of Absorption Lines (0.1 nm)

Name	K CaII	H $\delta$	CN	G band	H $\gamma$	H $\beta$	MgI+MgH
NGC 2537	18.96	2.293	5.692	3.329	-14.7	-33.9	4.270
Mrk 19	9.878	5.313	-0.37	3.786	-4.21	-35.5	4.138
Mrk 108	18.25	-8.92	8.427	4.192	-37.1	-105.0	3.434
Mrk 25	4.318	3.482	3.954	2.682	-2.39	-8.96	2.895
Mrk 35	2.769	-6.29	7.278	1.936	-15.1	-22.6	3.375
UGC 9560	4.736	-4.67	4.230	3.678	-10.7	-40.5	4.303
UGCA 410	10.61	1.073	14.33	8.688	-13.0	-50.6	3.237

### 3. STELLAR POPULATION SYNTHESIS METHOD

To study the star formation regime, the age and the distribution of invisible matter of BCDG, we applied the population synthesis method of Bica (1988)<sup>[16]</sup>, based on star cluster spectra samples, to study the stellar population component in its nuclear region. This method uses as criteria, a set of strong, certain and readily distinguishable characteristic absorption lines that are strongly correlated with age and metallicity. By comparing the equivalent widths of these observed lines with the synthetic lines resulting from a trial composition of the star cluster spectra sample, we try to derive the contributions of different stellar components with different age and metallicity to the galaxy<sup>[16–18]</sup>.

Compared to population syntheses based on stellar library and evolutionary population synthesis, this method has some merits. First, the number of variables is reduced, only two parameters are needed: age and metallicity. Second, compared to stellar spectra, star cluster spectra have fewer varieties, which makes the observation and calculation easier. Lastly, the star cluster method does not require information on the initial mass function and stellar evolution;—these are implicit in the cluster data. Considering that there probably exist some uncertainties due to observational error and incompleteness of sample, the algorithm is a multi-minimization procedure, which finds valid solutions within some error range, not just a single optimal solution. Then we use a statistical method to obtain a final, average solution. Because of these merits, this method is now widely applied to emission line galaxies and normal galaxies<sup>[19–21]</sup>.

The computation can be performed in two ways: one way spans the whole age-metallicity plane (multi-minimization procedure, hereafter MMP) while the other is restricted to chemical evolutionary paths in the age-metallicity plane (direct combination procedure, hereafter DCP). We combine these two procedures in our paper. We first use the MMP method to single out the main contributing components, and then, based on their resemblance to the whole-plane solution and on their reduced  $\chi^2$ , we select the best evolutionary path and use the DCP method to give the final result. The method greatly reduces the possibility of arbitrary assumption on the evolutionary path, gives at the same time the evolutionary sequence of the stars inside the galaxy, and overcomes the shortcomings of the MMP and DCP by themselves.

## 4. POPULATION SYNTHESIS OF SPECTRA

### 4.1 The Result of the Multi-Minimization Procedure (MMP)

In this procedure we try various combinations of all components in the “age-metallicity plane” until a good fit between the equivalent widths of the resulting lines and the observed lines is obtained. The number of cluster sample is 35, the serial numbers 1–35 representing these components, in Table 4a. In Table 4, the first line specifies the age of the component in units of  $10^6$  yr, the ninth column,  $[Z/Z_{\odot}]$ , gives the logarithm of its metallicity in solar units. In addition, RH represents a featureless continuum that quantifies the effect of internal reddening on the continuum and is independent of its metallicity.

This method allows sweeping through the vector space of solutions generated by the 35 component basis in a fast and efficient way, leading to a representative set of acceptable solutions to the synthesis problem. We tried various combinations of the 35 components until a good fit between the equivalent widths of the synthetic and observed lines is obtained. An iterative optimization procedure was used, each iteration altering the percentages of the components. The input parameters are the measured equivalent widths of selected absorption lines and the continuum. The results are expressed in terms of flux fractions at 587.0 nm for each component in the average solution and are displayed in Tables 4b–4h.

From the results of the multi-minimization procedure, we can find some obvious characters for each of the galaxies. First, there are very few old ( $t > 10^{10}$  yr) and high-metallicity ( $Z/Z_{\odot} \geq 0$ ) globular clusters, while old and low-metallicity globular clusters are much more



#### 4.2 Results of Direct Combination Procedure (DCP)

To avoid and reduce the dispersion, all the population synthesis methods so far made presupposed some arbitrarily chosen chemical evolutionary path in the age-metallicity plane. The improvement introduced by our method is this: we shall pick out from the MMP result those components that contribute importantly and use them to define the path of chemical evolution, thus reducing the degree of arbitrariness of choice. We find the main contribution comes from middle age and young star clusters at metallicity  $Z/Z_{\odot} = 0.0$  in the MMP results. A path containing 12 components, along the time sequence  $T = 10^7 \sim 5 \times 10^9 \text{yr}$  at fixed metallicity  $[Z/Z_{\odot}] = 0.0$ , and then along the metallicity sequence  $[Z/Z_{\odot}] = 0.0 \sim -2.0$  with  $t > 10^{10} \text{yr}$ , plus the HII region was used for the DCP method. The rationale of this path can be found in Ref. [15].

The path solution is given in Table 5. The heading of Table 5 is the serial numbers of the star clusters in the age-metallicity plane. The results for each BCDG are expressed in terms of flux fractions at 587.0 nm of the components in the average solution. We can note some obvious features in Table 5. We see that the stellar components with age  $t = 5 \times 10^7 - 10^9 \text{yr}$  make a dominant contribution,  $\geq 50\%$ , and the old globular clusters components make sizeable contributions. The indication is that an enhanced star formation event occurred at that epoch. The other obvious feature is that the youngest component ( $t = 10^7 \text{yr}$ ) is not important, which possibly suggests that the star formation rate had decreased by then. The old globular clusters components have different values in different galaxies, which are generally lower than for the middle age and young stellar populations. It suggests that star formation did occur at the early stage but the rate was not high;—this is similar to the MMP results. The HII region is a featureless continuum, which acts in the synthesis as a dilutor of absorption lines. From Table 5, we can find that for BCDGs with intense star formation, the contribution from HII regions is small; it suggests that intense starbursts transfer gas into the stars. For the other BCDGs, in which star formation is not violent, the contribution from HII regions is important. The details of star formation are different in different galaxies, possibly this is the reason for the great diversity of morphology among the BCDGs.

**Table 5** The DCP Results of Stellar Population Synthesis for the BCDGs

Name	7	6	5	4	3	10	19	21	25	29	33	RH
NGC 2537	5.99	7.87	8.31	7.62	4.37	9.59	15.2	26.3	6.29	5.75	2.73	0.02
Mrk 19	2.22	0.66	2.47	1.44	2.67	4.24	10.7	52.4	12.2	8.93	1.81	0.25
Mrk 108	0.21	0.21	1.08	1.40	2.47	10.0	32.4	44.1	3.66	3.66	0.86	0.00
Mrk 25	4.38	4.33	3.75	3.88	3.87	6.70	12.1	19.8	9.40	7.17	2.10	22.5
Mrk 35	0.41	0.47	0.94	0.73	0.61	2.80	7.49	18.6	21.1	21.9	8.57	16.5
UGC 9560	0.73	1.16	1.72	2.47	3.69	11.4	14.7	15.0	7.26	8.01	4.28	29.5
UGCA 410	12.2	9.92	4.81	2.55	0.93	6.16	19.3	28.5	2.30	2.63	0.66	9.99

From our analysis of the stellar composition of BCDGs, we clearly see that they are old galaxies. Star formation did happen at the early stage with the formation of an old and metal-poor stellar population. Then, due to some internal or external factor, intense star formation was triggered, and lots of star formed. These stars result in the blue color and strong emission line spectrum of BCDGs. Now, the rate of star formation has decreased,

the luminosity is low, and dwarf galaxies have resulted.

## 5. DISCUSSION

### 5.1 Synthesized Spectra

In the previous Section, we applied the stellar population synthesis method to 7 BCDGs, the results give the contribution from different age and metallicity stellar population to the galaxy spectra. We now display the synthesis results for each galaxy in Figure 1, showing the percentage fluxes from the various stellar components: OGC for old globular cluster ( $t > 10^{10}$ yr), HIIr for HII regions, IYC for intermediate age star cluster ( $t \approx 10^9 - 5 \times 10^9$ yr), YBC for young blue star cluster ( $t \approx 10^7 \sim 5 \times 10^8$ yr). SYN represents the sum of all the previous components and OBS, the observed spectrum of the galaxy, displaced by the indicated amount. The emission line spectrum (OBS-SYN) resulting from subtracting SYN from OBS, is shown in the lower panels.

The figure shows that the synthesized spectrum gives a good fit to the observed continuum and absorption lines for each galaxy. It shows that the continuum of BCDGs comes mainly from the stars (particularly the young and intermediate-age stars) and HII regions and indicates that the main energy source of BCDGs is young, hot O, B stars, which give rise to HII regions around them. The observed emission line intensities are affected by underlying stellar absorption, which is different for different galaxies and different spectral lines. If we do not remove the stellar absorption contribution from the spectrum, it will affect substantially some of the emission lines used for the derivation of reddening and other physical and chemical parameters and the results will not be precise or even credible.

Another feature in Fig.1 is the obvious UV turn-up in the observed spectrum. The synthesized spectrum can fit it, but the fit is not perfect. Bressan et al. (1994) applied an evolutionary population synthesis method to the UV spectra, and found that the main sources of the UV turn-up are the young stars, the old hot horizontal-branch and asymptotic giant branch *manqué* stars of high metallicity, the latter being especially important<sup>[22]</sup>. In our Galaxy, these high metallicity stars are mainly located in the high-absorption galactic disk. In other galaxies, the individual stars cannot be resolved easily. So observation of these high metallicity stars is very difficult. Because the sample of population synthesis lacks these high metallicity stars or star clusters, the synthetic spectra do not give a good fit to the UV turn-up. A possible method is that we use the high-metallicity single stellar population (SSP, calculated from the evolutionary population synthesis method) to complete the sample of star cluster, and then use this complete star cluster sample to fit the galaxy spectrum.

### 5.2 Internal Reddening

Internal reddening is a thorny problem among other astrophysical problems. It is even more difficult when we deal with external galaxies<sup>[23]</sup>. In this paper, we will use the continuum and emission lines to make separate calculations of the internal reddening in the BCDGs.

In the method of population synthesis used in this paper, the internal reddening is taken as an adjustable parameter, so that an estimate for the internal reddening is made at the same time as the stellar populations. The method was described in Ref. [15]. This is an



empirical way of determining the internal reddening, its advantage is that it is assumption-free. The values of galactic internal reddening resulting from stellar population synthesis method are given in the second and third lines of Table 6.  $E(B - V)_{MMP}$  is the result from the MMP method,  $E(B - V)_{DCP}$  is the result from the DCP method.

The Balmer line ratio  $H_\alpha/H_\beta$  allows us to characterize the internal reddening in the regions where the nebular lines are produced. For those galaxies with  $H_\alpha/H_\beta$  greater than 2.88, we calculate the internal reddening by this line ratio. The difference in optical depths between the two emission lines  $H_\alpha$  and  $H_\beta$  is given by  $\tau_B^I$ ,  $\tau_B^I = \tau_\beta - \tau_\alpha = \ln \frac{H_\alpha/H_\beta}{2.88}$ , and  $E(B - V)_{H_\alpha/H_\beta} \approx 0.935\tau_B^I$ . In these formulae, three assumptions are implicit, Case B recombination, the extinction law for our Galaxy and even dust distribution around the nucleus. The results are presented in the last two lines of Table 6, calculated from the spectral line ratio without and with the correction for the underlying stellar absorption.

**Table 6** The Internal Reddening of the BCDGs

Internal Reddening	NGC 2537	Mrk 19	Mrk 108	Mrk 25	Mrk 35	UGC 9560	UGCA 410
$E(B - V)_{MMP}$	0.13	0.03	0.03	0.06	0.05	0.03	0.02
$E(B - V)_{DCP}$	0.12	0.03	0.03	0.04	0.04	0.02	0.02
$E(B - V)_{H_\alpha/H_\beta}$	/	0.16	0.29	0.28	0.11	0.20	0.28
$E(B - V)_{S-H_\alpha/H_\beta}$	/	0.10	0.13	0.16	0.09	0.15	0.24

From Table 6, we find the internal reddening to be clearly dependent on the shape of the spectrum: the flattest spectrum (NGC2537) goes with the largest color excess, the steepest spectrum, the least internal reddening. We find also that the values are small, which is consistent with the BCDGs being metal-poor and dust-poor. In addition, we find that the internal reddening of the stellar continuum in BCDGs is generally lower than that of ionized gas. A model of foreground clumpy dust, with different covering factors for gas and stars, is a possible explanation for the difference. The covering factor by dusty clumps is greater for the gas regions that generate the emission lines than for the stars that produce the continuum. This difference may have resulted from the following circumstance: the formed massive stars end their lives in a short time and violently, throwing the dust in their region of their formation into the emission line regions. That the continuum emission of stars are less obscured than are the emission lines of ionized gas, has been pointed out for other kinds of emission line galaxies<sup>[14-15]</sup>.

### 5.3 Evolution among Dwarf Galaxies

Because the observational characteristics of blue compact galaxies (BCGs) and BCDGs are very similar, such as the blue color, strong and narrow spectral lines, most of us think that their difference is only a difference in  $M_B$ . In this paper, we know the stellar component of BCDGs by the population synthesis method. In our other paper<sup>[15]</sup>, we have discussed the stellar component of BCG. We will now compare the results to bring out their differences.

The similar characteristics are: 1) The star formation happen in short intense bursts, separated by long quiescent phases. 2) They are old galaxies, star formation happened already at an early stage. 3) The synthesized spectrum gives a good fit to the observed continuum and absorption lines. 4) The internal reddening value is small in both cases, and it is generally lower for the stellar continuum than for the ionized gas.

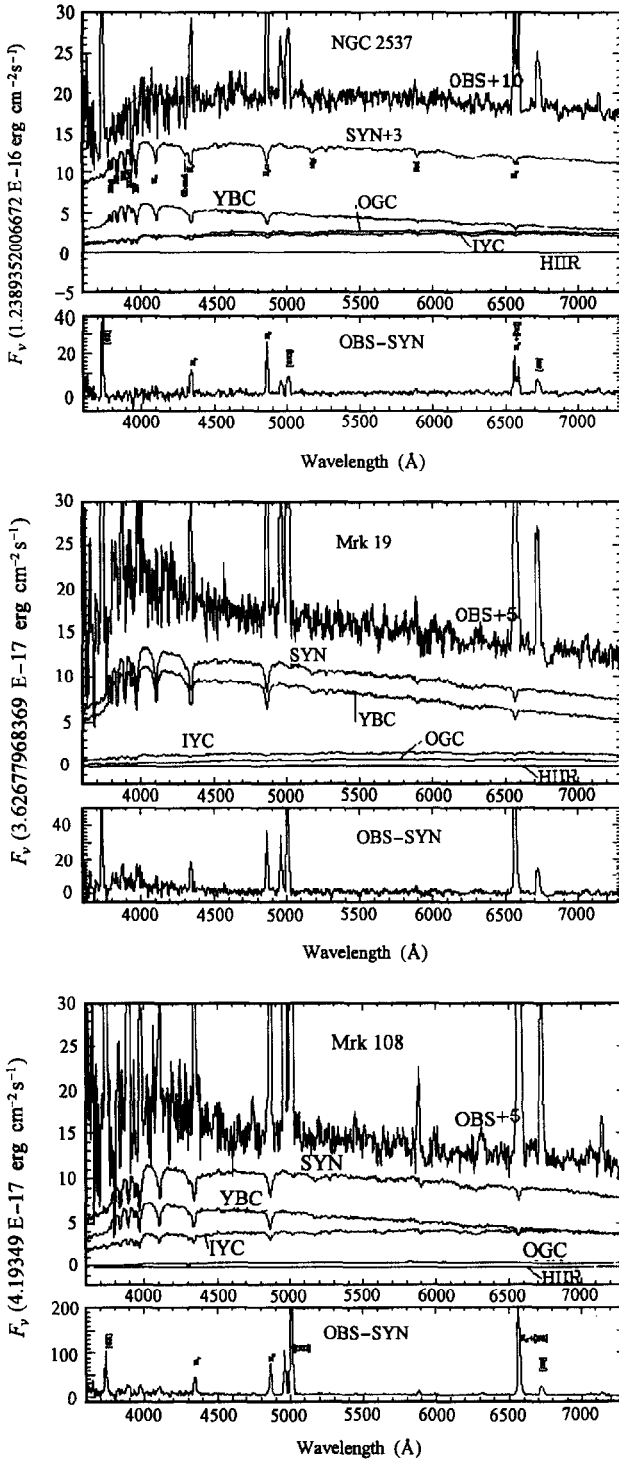


Fig. 1 The stellar population synthesis spectra of BCDGs

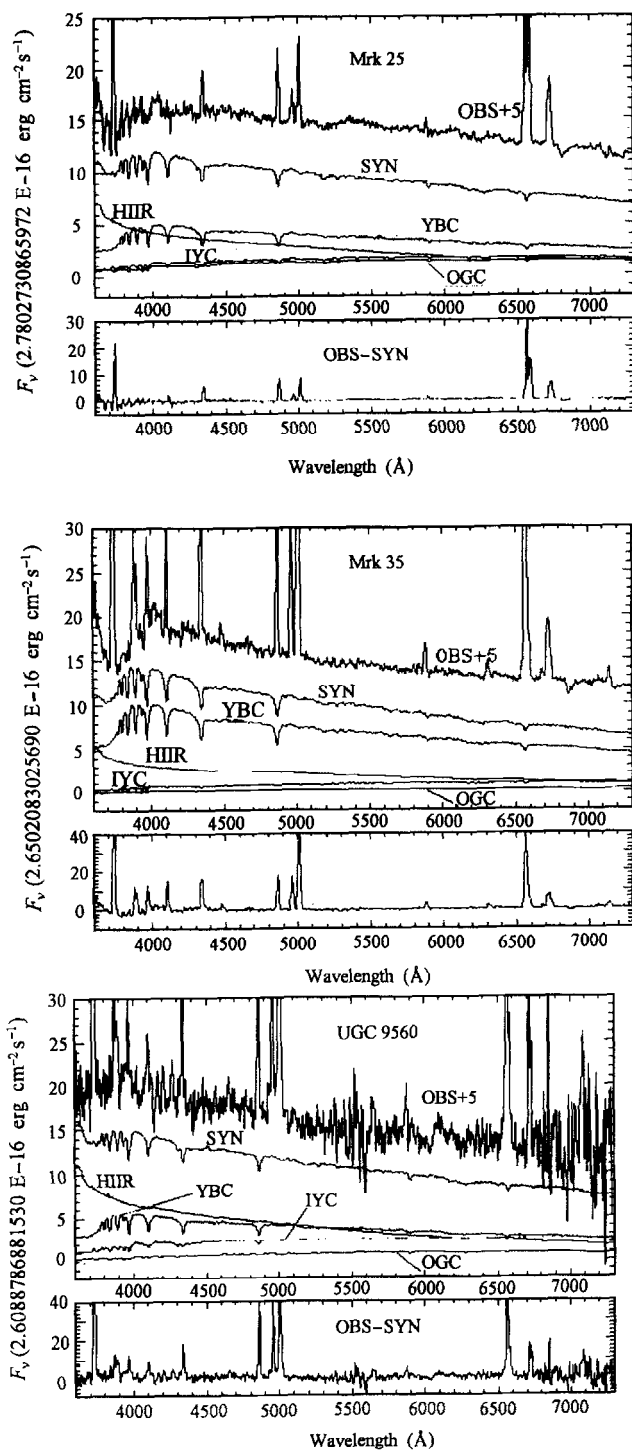


Fig.1 (cont.)

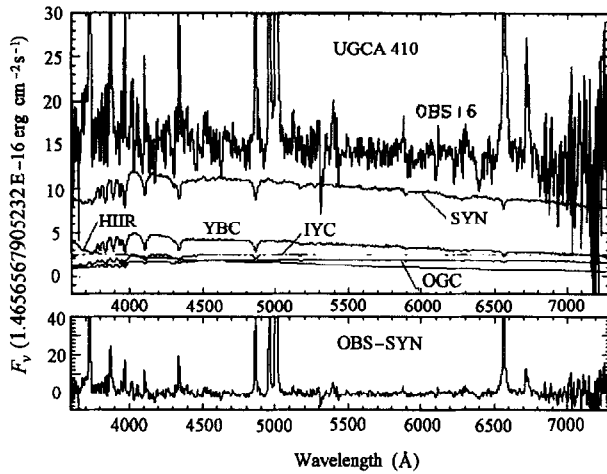


Fig. 1 (cont.)

While BCGs and BCDGs have those properties in common, their stellar components and star formation regimes are generally different. The BCGs have lots of old and young stellar components and their recent star formation rate is very high. For BCDGs, on the other hand, the old and young stellar components are relatively smaller, and the contribution from intermediate age stellar population is important. The population synthesis results suggest some evolutionary relation between the high surface brightness BCGs and BCDGs. Moreover, the existence of old stellar component in the majority of BCGs supports the argument that they are not truly primordial galaxies, rather, they are older dwarf galaxies undergoing transient periods of star formation. There may exist an evolutionary scenario involving the BCGs and other dwarf galaxies, such as dwarf irregulars (dIs), dwarf ellipticals (dEs). A specific evolutionary link, such as dIs  $\rightarrow$  SBs  $\rightarrow$  BCDGs  $\rightarrow$  high surface brightness BCGs  $\rightarrow$  dEs, may exist among these galaxies.

In this scenario, initially, the overall gas density is assumed to be below the threshold density for massive star formation, so the dI may contain just a few OB associations, and be in a relatively quiescent stage. The gas component experiences the gravitational forces from the stellar component and from itself, and as long as angular momentum can be neglected, it will contract, the gas accumulates gradually, and when the gas attains eventually a density high enough to allow massive star formation, the first starburst is initiated, transforming the dI to an SB. Supernova-driven winds will expel the gas and halt the star formation, and as the amount of gas decreases from stripping, the SB, at the end of violent starburst activity, fades to form a BCDG. The hot gas left over from the first starburst era is trapped in the surrounding halo of the galaxy, falls inward, cools and is accreted on to the BCDG again. Following the gas infall from the halo, a second star formation burst is triggered. As a result, the BCDG is transformed into a high surface brightness BCG (the second burst). When the gas reservoir for star formation is exhausted in several such starbursts, the galaxy fades from its last BCG stage into a gas-poor dE, with a decreased luminosity and surface brightness; thus, at the end of the starburst activity, a high surface brightness BCG fades to form a compact dE. This evolutionary link agrees with the results from a galaxy morphology study<sup>[24]</sup>.

## 6. SUMMARY

We have observed the nuclear region spectra of 7 blue compact dwarf galaxies, using the 2.16-m telescope of the Beijing Astronomical Observatory. We have applied to these spectra a population synthesis method which uses a base of star cluster integrated spectra and reached the following conclusions:

- 1) BCDGs are old galaxies: star formation did occur at an early stage.
- 2) The process of star formation in BCDGs is intermittent, the star formation is very violent during  $t = 5 \times 10^7 \sim 10^9$  yr.
- 3) A good fit can be achieved between the synthesized and observed continuum spectrum, which possibly suggests that the stellar component is an important energy source for BCDGs.
- 4) Comparing the internal reddening values derived separately from the continuum and emission lines, we can conclude that the continuum and emission line regions have different degrees of obscuration from dust. These region may be separate in space.
- 5) Based on the stellar population and star formation regime in BCDGs, we suggest a detailed evolutionary link among different types of dwarf galaxies.
- 6) We have derived emission line spectra freed from the effect of the stellar component and internal reddening; these should be useful for the investigation of physical conditions and chemical abundance of the emission line region of BCDGs.

## References

- 1 Sung E. C., Han C., Chun M. S. et al., *ApJ*, 1998, 505, 199
- 2 Zwicky F., *Advances in A&A*, New York: Academic Press, 1967, 5, 267
- 3 Zwicky F., *Catalogue of Selected Compact Galaxies and of Past-Eruptive Galaxies*, 1971
- 4 Doublier V., Comte G., Petrosian A. et al., *Ap&SS*, 1997, 124, 405
- 5 Hunter D. A., Thronson JR. H. A., *ApJ*, 1995, 452, 238
- 6 Sage L. J., Salzer J. J., Loose H. H., *A&A*, 1992, 265, 19
- 7 Kinney A. L., Bohlin R. C., Calzetti D. et al., *ApJS*, 1993, 86, 5
- 8 Thuan T. X., Martin G. E., *ApJ*, 1981, 247, 823
- 9 Izotov Y. I., Thuan T. X., Lipovetsky V. L., *ApJS*, 1997, 108, 1
- 10 Krueer H., Fritze-V. Alvensleben U., Loose H. -H., *A&A*, 1995, 303, 41
- 11 Thuan T. X., Izotov Y. I., Lipovetsky V. A., *ApJ*, 1995, 445, 108
- 12 Thuan T. X., Izotov Y. I., Lipovetsky V. A., *ApJ*, 1996, 463, 120
- 13 Garnett D. R., Skillman E. D., Dufour R. J. et al., *ApJ*, 1997, 481, 174
- 14 Calzetti D., *AJ*, 1997, 113, 162
- 15 Kong X., Cheng F. Z., *Chin. Astron. Astrophys.*, 1998, 22, 145
- 16 Bica E., *A&A*, 1988, 195, 76
- 17 Schmitt H. R., Bica E., Pastoriza M. G., *MNRAS*, 1996, 278, 965
- 18 Bonatto C., Bica E., Alloin D., *Ap&SS*, 1995, 112, 71
- 19 Winge C., Peterson B. M., Horne K. et al., *ApJ*, 1995, 445, 680
- 20 Storchi-Bergmann T., Bica E., Kinney A., Bonatto C., 1997, *MNRAS*, 290, 231
- 21 Cid Fernandes R., Storchi-Bergmann T., Schmitt H. R., *MNRAS*, 1998, 297, 579
- 22 Bressan A., Chiosi C., Fagotto F., *ApJS*, 1994, 94, 63
- 23 Ho L. C., Filippenko A. V., Sargent W.L.W., *ApJ*, 1997, 487, 579
- 24 Patterson R. J., Thuan T. X., *ApJS*, 1996, 107, 103